Charge transport measurement during turbulent electroconvection

J. T. Gleeson
Department of Physics, Kent State University, Kent, Ohio 44242
(Received 30 May 2000; published 26 January 2001)

We report measurements of the energy dissipation during electroconvection of a nematic liquid crystal in the fully turbulent regime. The energy dissipation is quantified by measuring the electric current at constant potential difference. In certain cases, we observe the surprising result that the dimensionless energy dissipation ceases to increase with increasing potential difference. In some circumstances, a power-law scaling relationship between the dimensionless excess energy dissipation and the reduced voltage is observed, but the exponent in this relationship varies dramatically with both the time scale of the driving electric field and the separation between the electrodes.

DOI: 10.1103/PhysRevE.63.026306 PACS number(s): 47.27.−i, 61.30.−v, 47.27.Te

I. INTRODUCTION

Electroconvection in nematic liquid crystals is in many ways analogous to the more familiar phenomenon of Rayleigh-Bénard (or thermal) convection. In thermal convection, a temperature gradient, antiparallel to the gravitational force, is maintained across a fluid layer. When the thermal gradient, expressed in terms of the dimensionless Rayleigh number R exceeds a critical value (R_c), convective flow spontaneously arises. [1] As the Rayleigh number is increased above R_c, a cascade of secondary instabilities is observed, leading to fully developed turbulence at values of R above about 10^4. Strongly disordered flow in thermal convection has been extensively studied for many years, and has led to a substantially enhanced understanding of the thorny problem of turbulence in general. Much attention has been focused on calculating and measuring the heat transport during turbulent thermal convection. Specifically, one finds a power-law scaling behavior, in which the total heat transported is found to be proportional to R^α over several decades in R. [2,3] Calculating and measuring the exponent α has been the principal focus of this previous work. Recent precise results [4] shows that a single power law is not completely sufficient to describe the energy transport.

Electroconvection in liquid crystals can arise when the liquid crystal is subject to stress not in the form of a temperature gradient, but a gradient of the electric potential. Under the proper conditions, when the rms potential difference V across a nematic liquid crystal exceeds a critical value V_c, flow arises spontaneously. As a nonlinear dynamical system, this has been intensely studied for over 30 years. [5] Although there are many similarities between Rayleigh-Bénard convection in simple fluids and electroconvection in liquid crystals, energy transport measurements in electroconvection have been surprisingly rare. We recently completed a study of energy transport during electroconvection. [6] This study focused on the weakly nonlinear regime just above the onset of convection. In this paper we instead concentrate on the so-called ''dynamic scattering'' [7] turbulent regime that results when V greatly exceeds V_c.

One reason for the paucity of studies of the high V regime is the immense difficulty this strongly turbulent regime presents for optical studies. Because liquid crystals are birefringent, in the dynamic scattering regime the optical axis is rapidly randomized, leading to extremely strong depolarizing scattering of light. For $V=10V_c$, the optical density of a 25 μm thick liquid crystal undergoing dynamic scattering is greater than 1.5; our measurements extend to $V>60V_c$. Thus, the traditional shadowgraph [8] technique is of no use in this regime. For this reason we have chosen to concentrate on energy transport studies enabled by measuring the electric current induced by an potential difference sufficient to induce turbulent electroconvection in a nematic liquid crystal.

In Rayleigh-Bénard convection, the amount of energy transport is characterized by defining a thermal Nusselt number. This is the ratio of heat transported between the lower and upper bounding surfaces of the fluid relative to the heat transport in the absence of flow (the so-called conductive regime, or quiescent state). In electroconvection, the analogue of heat transport is charge transport. The potential difference across the conducting plates bounding the nematic liquid crystal has the form $V(t)=\sqrt{2}V\cos(\omega t)$. The in-phase component of the current due to this potential difference is $I(t)=\sqrt{2}I\cos(\omega t)$. We define the electrical Nusselt number Nu as I/I_0, where I_0 is $V/R_\perp$, the current amplitude in the absence of convection. $R_\perp$ is the resistance of the nematic liquid crystal in the quiescent state. With this definition, the excess energy dissipation in the nematic liquid crystal due to convection is $V^2(\mathrm{Nu}-1)/R_\perp$. An additional Nusselt number can also be defined based on the out-of-phase current, $I(t)=\sqrt{2}I_i\sin(\omega t)$; this Nusselt number is not relevant for energy transport, and we do not consider it further here. Sometimes, the results of experiments such as these are expressed in terms of a reduced Nusselt number, defined as $\mathrm{Nu}-1$.

Studies of energy transport in Rayleigh-Bénard convection present the Nusselt number as a function of R; recall that R must exceed $R_c=1708$ to induce convection. In order for comparisons between our electroconvection results and those from Rayleigh-Bénard to be useful, results must be presented in terms of a reduced control parameter; for Rayleigh-Bénard, one defines the reduced Rayleigh number $r\equiv R/R_c$; for electroconvection we use the reduced voltage $v\equiv V^2/V_c^2$.

II. EXPERIMENT

The ''classical'' experimental arrangement is employed [9]. The nematic liquid crystal is confined between transpar-

ent conducting planes in the parallel-plate capacitor geometry. The plates are indium-tin-oxide coated borosilicate glass plates. The indium tin oxide has been selectively etched to provide an ''active area'' in the center of the sample. Outside the active area, there is no conductive coating and so no electric field is present. The parallel plates have also been unidirectionally rubbed to induce planar alignment of the nematic director parallel to a single direction in the quiescent state. After the plates are prepared, they are glued together with spacers interposed between them to control their separation d. For the experiments reported here, different samples were prepared in which d varied between 22.7 μm and 227 μm. After gluing, the nematic liquid crystal methoxy benzylidene-butyl aniline (MBBA), doped with 0.0005% tetrabutyl ammonium bromide is introduced between the plates via capillary action. This liquid-crystal preparation had a cutoff [5] frequency of 495 ± 11 Hz. Electrical contacts are made to the conducting areas via silver epoxy.

Energy transport is quantified by measuring both the potential difference across and the electrical current through the nematic liquid crystal. A function generator produces a sinusoidal voltage signal that is amplified and applied across the liquid crystal layer. The path to ground for the current traversing the layer is through the field-effect transistor input of a current-to-voltage converting preamplifer. The output of this preamplifier is measured by a lock-in amplifier. The reference signal for this amplifier is supplied by the original function generator. Before any measurements are made, the liquid-crystal cell is replaced by a purely resistive load, and the phase angle of the lock-in is adjusted to zero the out-of-phase component.

The nematic cell is reinserted. At a selected frequency V is raised in small steps; after a waiting period the current is measured. The waiting period is chosen to be at least as large as the director diffusion time: $\tau_d \equiv d^2 \gamma_1 / K_1 \pi^2$ [10]; γ_1 is the rotational viscosity, and K_1 is the splay elastic constant. For values of V well below V_c, $I_0 = V/R_\perp$; the low V data is fit to this relationship to obtain $R_\perp$. We then define Nu as $R_\perp I/V$. The value of V where Nu increases above unity is V_c; our previous studies [6] confirmed that V_c obtained this way agrees with that determined from traditional shadowgraph techniques within 0.01%.

Applying potential differences up to 400 V_{rms} across thin layers of nematic liquid crystal raises two potential problems that cannot be ignored. The first is Joule heating inside the nematic liquid crystal, and the second is dielectric breakdown of the liquid crystal itself. We do not witness the latter. The dielectric strength of MBBA is 15V/μm [11]; we do approach this value, but never exceed it significantly. We have never observed breakdown during these experiments.

In order to minimize the effects of Joule heating, the liquid-crystal sample is housed in a copper block that is held at 18 ± 0.01°C. We desired a large difference between the sample temperature and the nematic isotropic transition temperature so as to minimize the temperature dependence of material parameters. Furthermore, we estimate, based on the thermal properties of the nematic liquid crystal and the glass confining plates, that in the worst case, the largest temperature increase expected is less than 1°C. For most cases, the expected temperature increase will be substantially smaller than this.

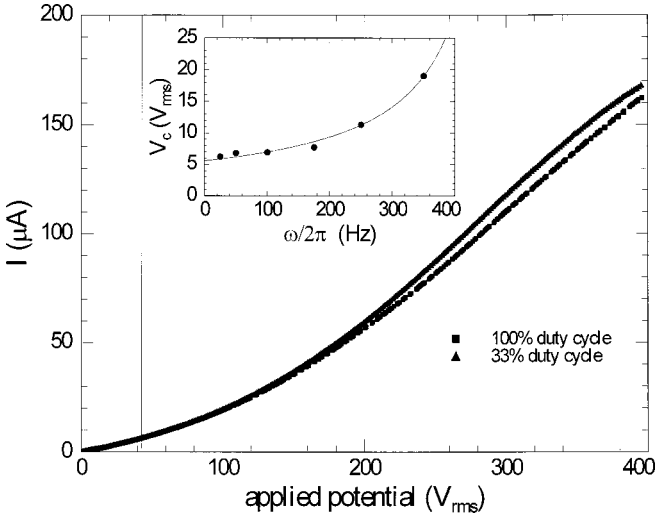

FIG. 1. Two examples of current-voltage data for electroconvection of the nematic liquid-crystal MBBA. The upper curve was obtained when the driving voltage was continually applied, and the lower when the driving voltage was applied for 5 s, then set to zero for 10 s. Inset: Critical voltage (V_c) vs frequency. The solid line is a fit to the prediction of the standard model [5] for electroconvection; this fit yields the cutoff frequency ω_c.

III. RESULTS

Our results on energy transport are obtained by measuring the I-V characteristics as described above. An example of I-V data is shown in Fig. 1. Since Joule heating is identified as a potential difficulty, its effect is also revealed in Fig. 1. This shows two I-V curves, one taken using a 100% duty cycle, where the drive voltage is always applied, and the other using a 33% duty cycle. In the latter case, the desired voltage was applied for 5 s, after which the current was measured, and the voltage was set to zero for 10 s, after which this cycle is repeated at the next higher voltage. The difference in current for these two cases never exceeds 6%, and the largest discrepancy does not occur at the largest voltage. Thus, we are confident that Joule heating does not present a significant problem.

The energy transport is quantified in a dimensionless manner via the Nusselt number. Using the method described above, the I-V data as in Fig. 1 is reduced to show Nu vs v; an example is shown in Fig. 2. In this figure, we see Nu saturating at about 3.2 at high v; this puzzling behavior is discussed subsequently. Since one goal is to investigate whether there exists a power-law scaling relationship between the Nusselt number and the reduced voltage, in Fig. 3 we plot Nu vs v using log-log axes. Figure 3 reveals several important features. First, over certain ranges of v, there are indeed indications of power-law scaling. In searching for scaling regimes, we arbitrarily restricted ourselves to examining ranges no smaller than one decade in v. The straight line drawn on Fig. 3 indicates such a regime. This regime

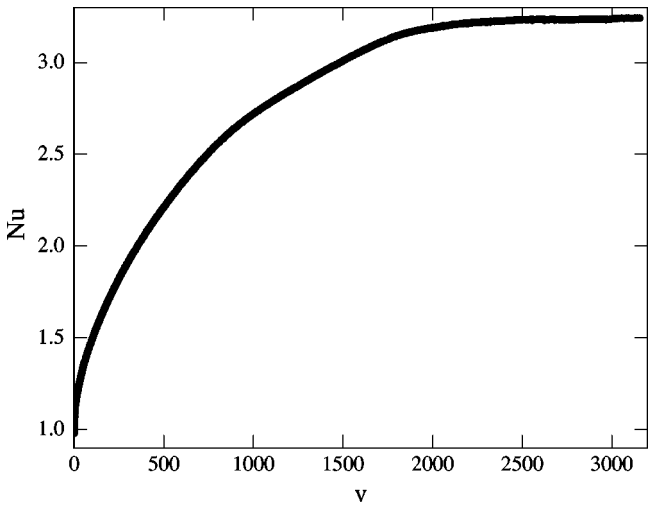

FIG. 2. Example of electrical Nusselt number vs reduced voltage for turbulent electroconvection. The saturation of Nu at high v can be observed for $v>2500$. In this example, the frequency $\omega/2\pi$ is 100 Hz, and the separation d is 22.7 μm.

corresponds to v ranging between about 175 to 17 500. To aid comparison, comparable Rayleigh numbers for Rayleigh-Bénard convection would be about 320 000 to 3 200 000. Thus, over this range, we find $\mathrm{Nu}\propto v^{\alpha}$, with $\alpha=0.281$. It must be noted that this range is not as large as typically seen in thermal convection; one possible reason that this scaling regime is shortened is discussed below. Experiments on Rayleigh-Bénard convection have shown scaling regimes for Rayleigh numbers as low as 10^4 and as high as 10^{12}; with exponents between 0.247 and 0.333, but clustered around 0.29. Thus, the scaling we observe here is indeed comparable to that observed in traditional thermal convection.

In thermal convection, the relevant time scale is dictated by the Prandtl number: the ratio of viscous diffusion to heat

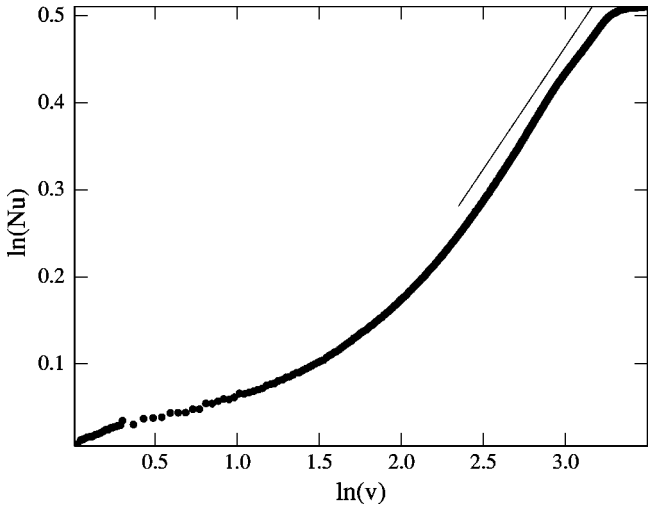

FIG. 3. Example of log-log plot of Nusselt number vs reduced voltage for turbulent electroconvection. The straight line shown has slope 0.281. The decade-wide interval from $v=172$ to 1720. Clearly, the saturation of Nu has serious consequences on the extent of power-law scaling regions.

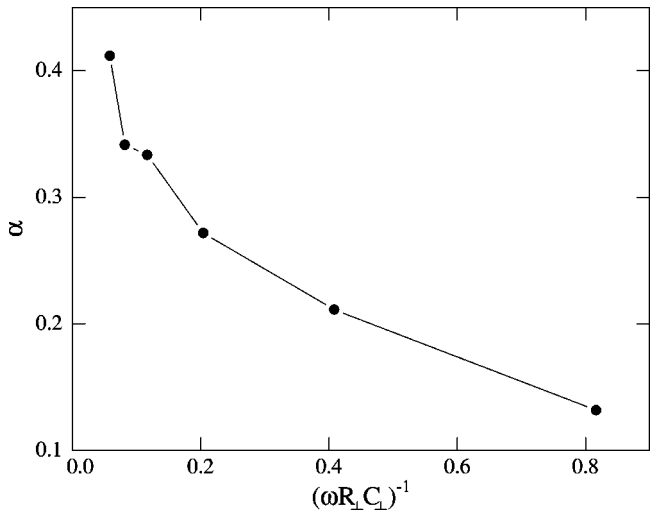

FIG. 4. Scaling exponent α vs ω^{-1} for turbulent electroconvection. The inverse frequency is made dimensionless by scaling with the charge relaxation time $R_{\perp}C_{\perp}$.

diffusion. For a wide range of Prandtl numbers (0.025–6), the exponent α does not deviate significantly from the value 0.29 reported above. In electroconvection, the relevant time scale is determined by the period of the applied electric field, made dimensionless by dividing by the charge relaxation time of the liquid crystal, $R_{\perp}C_{\perp}$, where $C_{\perp}$ is the capacitance of the quiescent state. Figure 4 shows the measured exponent α for electroconvection vs $1/\omega R_{\perp}C_{\perp}$. While this data does not span a large enough range to draw any conclusions about scaling with $1/\omega$, the tremendous variation in α is striking. In stark contrast to thermal convection, α changes by more than a factor of 3, ranging between values both greater and smaller than ever reported in thermal convection.

Interestingly, the transition from anisotropic convection to isotropic convection (the so-called DSM1-DSM2 transition) [12] has no apparent signature in the Nusselt number. The vertical line in Fig. 1 lies where this transition was (optically) observed. This transition evidently has no impact on energy dissipation.

IV. DISCUSSION

Figure 3 shows that power-law scaling indeed occurs. We have measured exponents that are both substantially larger and smaller than ever measured for Rayleigh-Bénard convection. Moreover, the exponent changes with the relevant time scale in a much more dramatic fashion than is observed in thermal convection. Beyond this demonstration of scaling, however, there are numerous unexplained issues.

Most significant is the manner in which the scaling regime shown in Fig. 3 ends; via the saturation of Nu at large v. We are unaware of another example of a driven, turbulent system where the rate of energy dissipation relative to the conduction state ceases to increase with the driving force. Indeed, for frequencies $\omega/2\pi$ less than 100 Hz, Nu apparently even decreases with v for $v>1500$. The reason for this saturation remains unclear. In liquid-crystal electroconvection, one important contribution to enhanced charge transport

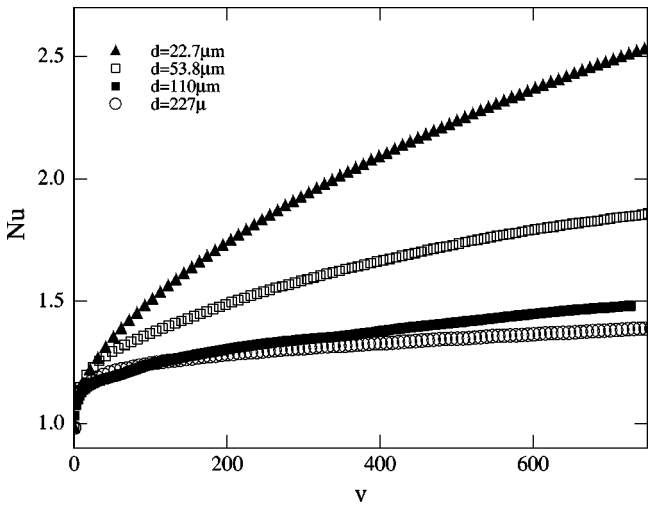

FIG. 5. Nusselt number vs v for different values of the electrode separation.

is the reorientation of the nematic director [13]. In the quiescent state, the conductance of the liquid-crystal layer is $d/A\sigma_{\perp}$, where A is the area of the conducting region. The maximum possible Ohmic conductance is $d/A\sigma_{\parallel}$. Thus, director reorientation alone can lead to a value of Nu no larger than $\sigma_{\parallel}/\sigma_{\perp}$. For the experiments reported here, this quantity is 1.35, far smaller than the saturation value above. The density of disclinations in the nematic director has been reported to saturate above the DSM1-DSM2 transition [14], but this saturation was observed at a far smaller potential difference than we see in the present paper. It is not known whether these two effects are related.

Also important is the manner in which Nusselt number depends on the separation between the electrodes. Again, we recall the analogy with Rayleigh-Bénard convection; in the turbulent regime, because the separation between confining surfaces is absorbed into the Rayleigh number, the Nusselt number's dependence on R does not change with d. Indeed, since $R \propto d^3$, varying d is a particularly effective way to span a wide range in R. Moreover, turbulent thermal convection is intimately associated with the formation of thermal boundary layers near the lower and upper surfaces. As these layers lose coherence with one another, the lower and upper surfaces become decoupled, and hence their separation ceases to be a relevant parameter. At higher Rayleigh numbers, a large scale mean circulation arises, which possesses its own length scale.

In contrast, the electrical Nusselt number exhibits a striking dependence on d. In Fig. 5 we show Nu vs v, at the same value of $\omega R_{\perp} C_{\perp}$, for values of d spanning almost an order of magnitude. The energy dissipation is at least twice as large, at the same r, for electrode separation 22.7 μm compared to 225 μm; thus, we see no indication of decoupled boundary layers in turbulent electroconvection. This dependence on d obviously has serious consequences for the scaling exponent α. For $d=227$ μm, α ranges between 0.026 and 0.040 as ω is changed, with no discernible, systematic dependence on ω. At $d=110$ μm, α is only slightly larger. In the so-called standard model of electroconvection, the electrode separation is normally chosen as the scale factor in which to rescale all other lengths. Within this model, after rescaling, the only role played by d comes in the ratio of the director diffusion time to the charge diffusion time. This ratio is essentially the parameter Q defined in Ref. [15], in which they also find that its value has little influence on the calculated results. As such, within this model, one expects no strong dependence on d when measuring rescaled quantities such as we have presented. However, we must stress that it is by no means certain that the mechanisms and descriptions of the standard model, developed to describe behavior just above the onset of convection, are applicable in this regime explored here. Indeed, the large density of disclinations in the director field significantly complicates any efforts to apply the standard model to this problem. The approach commonly used for flow in liquid-crystal polymers, in which the nematic order parameter is allowed to vary [16] may prove to be more amenable, because of the isotropic disclination cores.

One further important factor in Rayleigh-Bénard convection is the aspect ratio; the ratio of the lateral extent of the flow to the separation between the surfaces [17]. Indeed, one of the principal benefits of the electroconvection system for pattern formation studies are the relatively large aspect ratios possible. For the experiments reported here, the aspect ratio ranged from 220 to 22. However, this variation was due to the variation in d. Preparing experiments to systematically vary the aspect ratio at constant d is substantially more difficult.

V. CONCLUSIONS

Turbulent electroconvection indeed exhibits energy dissipation properties similar to those in high Rayleigh number thermal convection, but also reveals some unusual differences. For higher aspect ratios—smaller values of d, we observe Nusselt number scaling, with exponents that are comparable to those both observed and predicted for thermal convection. This scaling regime ends, and we find the rate of excess energy dissipation saturates, even as the driving force increases by 50%.

In sharp contrast to the case of thermal convection, we find a particularly strong dependence of the Nusselt number on either the aspect ratio or the plate separation. The reasons for this are unclear, especially in light of the standard theoretical description of electroconvection.

ACKNOWLEDGMENTS

We have benefited from discussions with G. Ahlers, E. Plaut, J. deBruyn, and M. Carme-Calderer. N. Gheorghiu assisted in preparing samples. This work was supported by Kent State University and the National Science Foundation, Grant No. DMR-9988614.

[1] S. Chandrasekhar, *Hydrodynamic and Hydromagnetic Stability* (Dover, New York, 1981).
[2] E.D. Siggia, Annu. Rev. Fluid Mech. **26**, 137 (1994).
[3] B. Castaing *et al.*, J. Fluid Mech. **204**, 1 (1989).
[4] X. Xu, K.M.S. Bajaj, and G. Ahlers, Phys. Rev. Lett. **84**, 4357 (2000).
[5] L. Kramer and W. Pesch, in *Pattern Formation in Liquid Crystals*, edited by A. Buka and L. Kramer (Springer-Verlag, New York, 1995).
[6] J.T. Gleeson, N. Gheorghiu, and E. Plaut (unpublished).
[7] G. Heilmeier, L.A. Zanoni, and L. Barton, Proc. IEEE **56**, 1162 (1968).
[8] S. Rasenat, G. Hartung, B. L. Winkler, and I. Rehberg, Exp. Fluids **7**, 412 (1989).
[9] A. Joets and R. Ribotta, Phys. Rev. Lett. **60**, 2164 (1988).
[10] P.G. deGennes and J. Prost, *The Physics of Liquid Crystals*, 2nd ed. (Clarendon, Oxford, 1993).
[11] L. Lam, R.D. Freimuth, and H.S. Lakkaraju, Mol. Cryst. Liq. Cryst. **199**, 249 (1991).
[12] S. Kai and K. Hirakawa, Suppl. Prog. Theor. Phys. **64**, 212 (1978).
[13] A similar contribution is seen in thermal convection of nematics. See L. Thomas, W. Pesch, and G. Ahlers, Phys. Rev. E **58**, 5885 (1998).
[14] S. Kai, W. Zimmermann, and M. Andoh, Mod. Phys. Lett. B **4**, 676 (1990).
[15] E. Plaut and W. Pesch, Phys. Rev. E **59**, 1747 (1999).
[16] See for example, M. Carme Calderer and B. Mukherjee, J. Rheol. **42**, 1519 (1998).
[17] X-Z. Wu and A. Libchaber, Phys. Rev. A **45**, 842 (1992).